Non-volatile memory device based on AgI-Ag_3BO_3 thin film

Xingcan Chen[1], Xuanxuan Cao[1], Chao Gu [2], Hui Jing [2], Ying Ding[1]

[1] Singapore Institute of Technology, Singapore 138682
[2] Lanzhou Jiaotong University, Lanzhou, Gansu, China, 730070

ABSTRACT

This work employs AgI-Ag_3BO_3 to fabricate nonvolatile memory device. First the AgI-Ag_3BO_3 amorphous material is prepared with quick cooling method. The thin film is grown onto Pt electrode with pulsed laser deposition. The resulting memory device presents a superiorly high difference between the low and high resistivity states, with a ratio above 10^6. In addition, the device shows a high stability after more than 10 thousand cycles. This structure may be used as a memory device with fast response and high stability.

Keywords *- nonvolatile memory, pulsed laser deposition, solid electrolyte, AgI-Ag_3BO_3*

I. INTRODUCTION

The rapid development of scale-down in the new era has advanced plenty of novel paradigms of designs, e.g., high performance electrical devices [1]. A straightforward method to work at small scale is to make the constituent materials smaller [2, 3]. Another approach is to find nanoscaled materials that as the elemental building blocks [4, 5]. Other tactics involve the infrastructures of multiple distinctly disparate ingredients to achieve functional properties at the macroscopic level [6-9]. The electrical equipment and electronics are experiencing revolutions in different fields [10-12]. For example, memories are needed almost everywhere in our daily life and work space, such as smart phones, computers, and servers. Due to the explosion of data, the demand for high performance and density memories are continuously increasing, approaching the final limit of Moore's law. In the last few decades, many endeavors have been put into the novel nonvolatile memory devices. Solid electrolyte materials attracted quite a lot of attention due to their unique characteristics that are superior or comparable with tradition materials [13-16]. A unique characteristic of solid electrolyte is that its resistivity may alter within a huge range, possibly 7 orders of magnitude. These distinct states of resistivity can be used as the „1" and „0" in memory devices. The successfully generated devices have shown superior performance compared with traditional equipment [17, 18].

In this work, a novel AgI-Ag_3BO_3 solid electrolyte system was generated to fabricate nonvolatile device. To the best of authors' knowledge, this system has not been applied before.

II. EXPERIMENTS

AgI, $AgNO_3$, and H_3BO_3 are thoroughly mixed with molar ratio 1:3:1 and ground into fine powders at room temperature (RT). The mixture is heated to 900 ˚C and kept for 2 hours. The chemical reaction is:

$$3AgNO_3 + H_3BO_3 = Ag_3BO_3 + \frac{3}{2}N_2O_5\uparrow + \frac{3}{2}H_2O\uparrow$$

The mixture is then quenched to RT into a bulk target with a chemical composition of 1:1 AgI-Ag_3BO_3.
Pulsed laser deposition was performed on the bulk target at a vacuum below 10^{-4} Pa. The laser fluence is 220 mJ with a frequency of 5 Hz. The total deposition time is 7 minutes.

III. RESULTS

3.1. Characterization

The XRD pattern (Fig. 1) shows that the generated material is apparently amorphous with a very small content of crystalline fractions. The characteristic peak with a circle is α-AgI, while the square is Ag(111). Among the two common phases of AgI, β-AgI has a lower conductivity than α-AgI. There have been a few reports on the applications of α-AgI, e.g., Tatsumisago et al. prepared nanocrystalline α-AgI in glassy networks at RT [19].

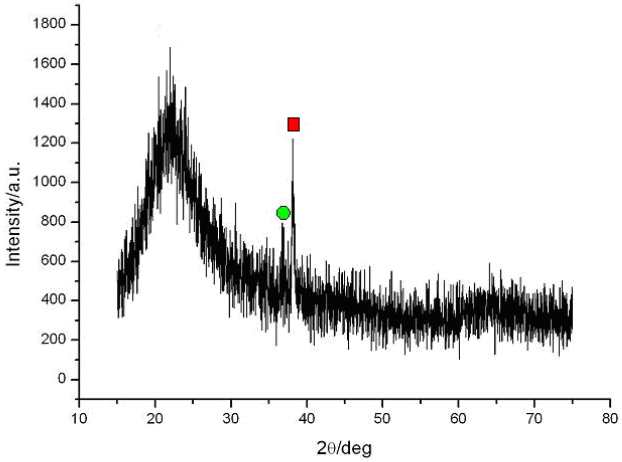

Fig. 1. XRPD pattern of the generated AgI-Ag_3BO_3

The generated thin film was examined under TEM and the image is presented in Fig. 2. Based on the image, the AIB thin film shows a morphology of nanocrystallites.

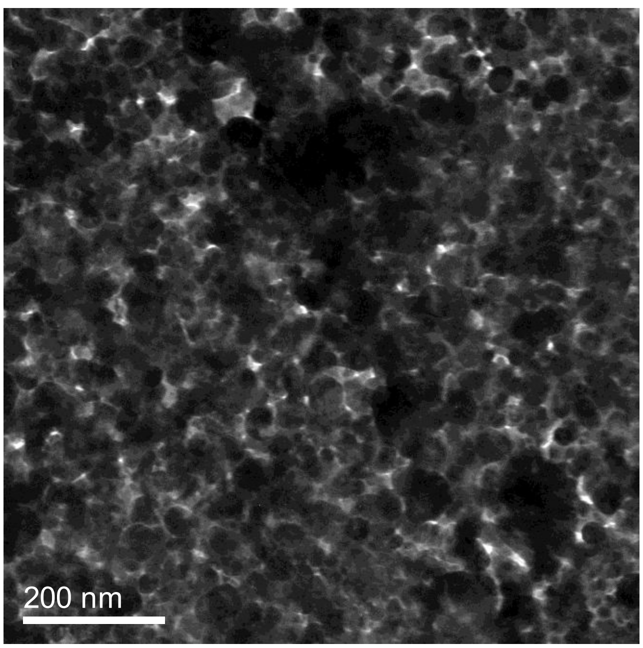

Fig. 2. TEM image of the AgI-Ag_3BO_3 thin film

The X-ray photoelectron spectroscopy (XPS) of the AgI-Ag_3BO_3 thin film is shown in Fig. 3. Based on the results, the Ag atom in the thin film is close to metal, indicating that it has a weak interaction with I. As a result, it may be easily converted to free Ag in electrical field.

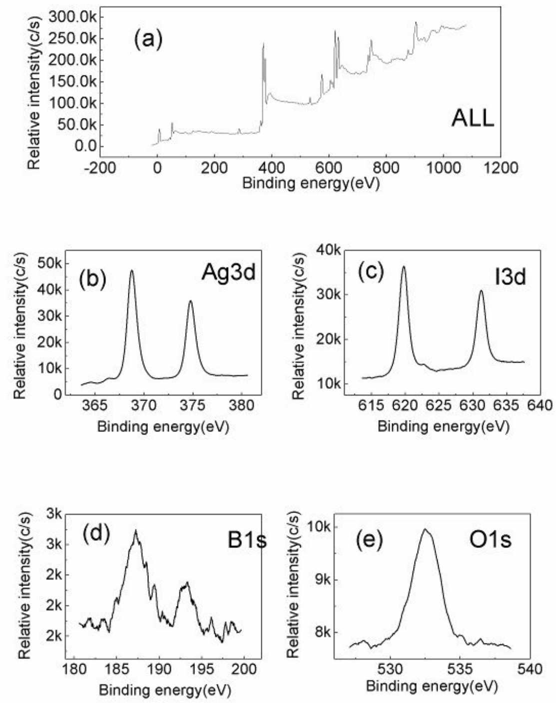

Fig. 3. XPS results of the AgI-Ag_3BO_3 thin film

Fig. 4 shows the structure of the final memory device based on AgI-Ag_3BO_3. The substrate at the bottom electrode is Pt and the top electrode is Ag. The thickness of Ag is about 100 nm and the AIB thin film is ~250 nm. The nonconductive SiO_2 was deposited on the Pt electrode and drilled with focused ion beam etching.

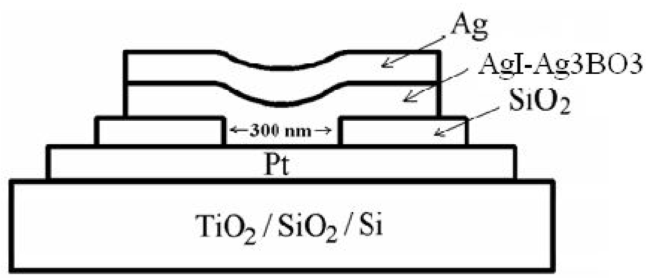

Fig. 4. Structure of the memory device based on AgI-Ag_3BO_3

The on/off switching effect of the memory device based on AgI-Ag_3BO_3 thin film is shown in Fig. 5. The ratio between high and low resistivity is above 10^6 and the device is cycled for more than 10^4 times.

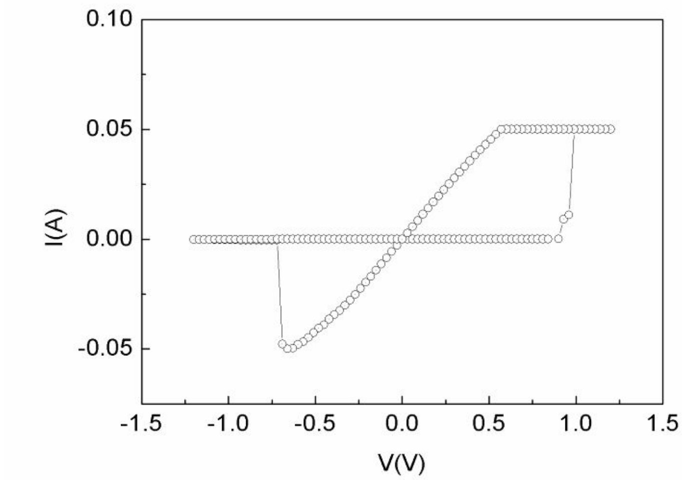

Fig. 5. The on/off switching of the memory device based on AIB thin film

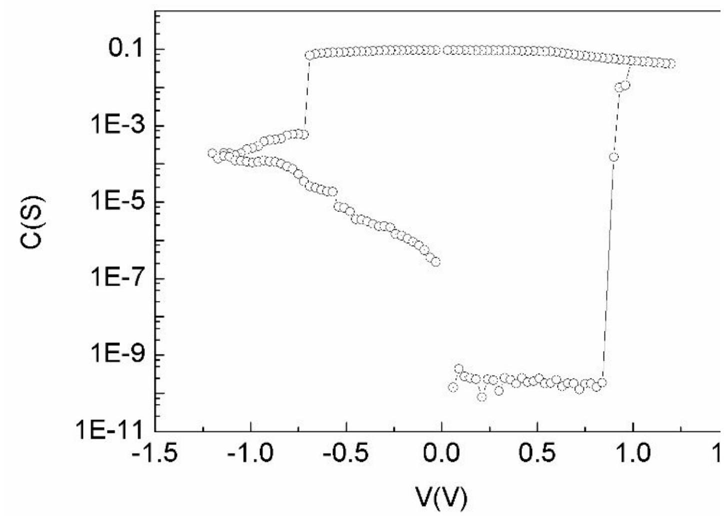

Fig. 6. Conductivity of the device under different voltages

Fig. 7 presents the on/off characteristics at the read-write pulse of 1 kHz. In each cycle, a positive voltage of 2.5 V as read pulse is applied to the device to enter the state of low resistivity; a negative voltage of 8 V as erase is applied to switch the device to the high resistivity state. Two pulses of read at 2 V are designated after write and erase. Between any two pulses, the voltage is 0. All pulses have a width of 0.125 ms and one full cycle is 1 ms. Based on the current which is 0 after read pulse, the state is high resistivity; while after write pulse, the current is approximately 11 mA, indicating the low resistivity state.

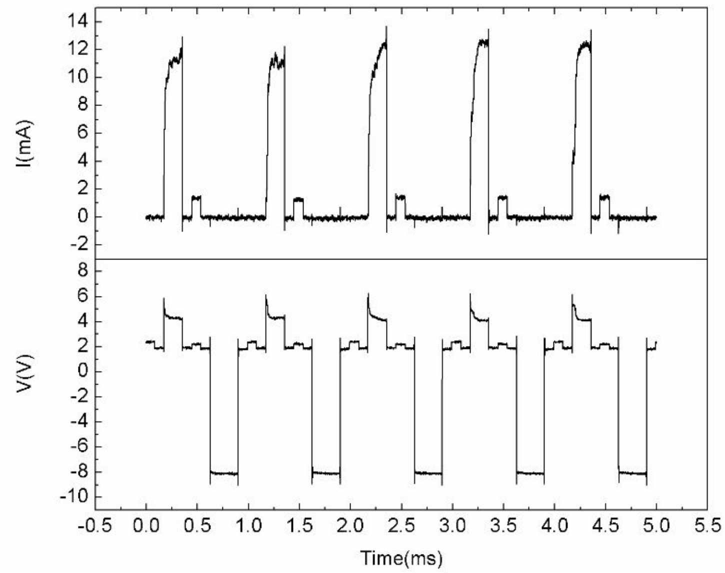

Fig. 7. AIB thin film device read-write cycles under 1 kHz

IV. CONCLUSION

This study prepares AgI-Ag_3BO_3 amorphous solid electrolyte via the quick cooling method. Then the AgI-Ag_3BO_3 thin film is grown onto Pt electrode with pulsed laser deposition. The resulting memory device shows a great difference between the low and high resistivity states, with a ratio above 10^6. In addition, the device shows a high stability after more than 10 thousand cycles. This infrastructured device may be used as a memory device with fast response and high stability.

REFERENCES

[1] W. Cai, F. Shi, DESIGN OF LOW POWER MEDICAL DEVICE, International Journal of VLSI design & Communication Systems (VLSICS), 8 (2017) 7.

[2] Y. Cao, P. Zavaterri, J. Youngblood, R. Moon, J. Weiss, The influence of cellulose nanocrystal additions on the performance of cement paste, Cement and Concrete Composites, 56 (2015) 11.

[3] K. Sobolev, Z. Lin, Y. Cao, H. Sun, I. Flores-Vivian, T. Rushing, T. Cummins, W.J. Weiss, The influence of mechanical activation by vibro-milling on the early-age hydration and strength development of cement, Cement and Concrete Composites, 71 (2016) 10.

[4] Q. Liu, J. Tian, W. Cui, P. Jiang, N. Cheng, A.M. Asiri, X. Sun, Carbon Nanotubes Decorated with CoP Nanocrystals: A Highly Active Non-Noble-Metal Nanohybrid Electrocatalyst for Hydrogen Evolution, Angewandte Chemie, 126 (2014) 5.

[5] Y. Cao, P. Zavattieri, J. Youngblood, R. Moon, J. Weiss, The relationship between cellulose nanocrystal

dispersion and strength, Construction and Building Materials, 119 (2016) 9.
[6] P.K. Jain, K. Manthiram, J.H. Engel, S.L. White, J.A. Faucheaux, A.P. Alivisatos, Doped Nanocrystals as Plasmonic Probes of Redox Chemistry, Angewandte Chemie International Edition, 52 (2013) 5.
[7] S. Gai, C. Li, P. Yang, J. Lin, Recent Progress in Rare Earth Micro/Nanocrystals: Soft Chemical Synthesis, Luminescent Properties, and Biomedical Applications, Chemical Reviews, 114 (2014) 47.
[8] Y. Cao, J. Weiss, J. Youngblood, R. Moon, P. Zavattieri, Performance-enhanced cementitious materials by cellulose nanocrystal additions, Production and Applications of Cellulose Nanomaterials, (2013) 2.
[9] W. Cai, F. Shi, Design of Low Power Si Based DPA for Medical Device, International Journal of Electronics Communication and Computer Engineering, 8 (2017) 3.
[10] W. Cai, L. Huang, N. Wu, Class E Power Amplifier for Wireless Medical Sensor Network, International Journal of Enhanced Research in Science, Technology & Engineering, 5 (2016) 6.
[11] W. Cai, L. Huang, W. Wen, 2.4GHZ Class AB Power Amplifier for Wireless Medical Sensor Network, International Journal of Enhanced Research in Science, Technology & Engineering, 5 (2016) 5.
[12] W. Cai, J. Gong, N. Wu, 2.4GHZ Class F Power Amplifier for Wireless Medical Sensor Network, Proceedings of the 2nd World Congress on New Technologies, (2016) 7.
[13] V.A. Agubra, J.W. Fergus, The formation and stability of the solid electrolyte interface on the graphite anode, Journal of Power Sources, 268 (2014) 10.
[14] J. Li, N.J. Dudney, J. Nanda, C. Liang, Artificial Solid Electrolyte Interphase To Address the Electrochemical Degradation of Silicon Electrodes, ACS Applied Materials & Interfaces, 6 (2014) 6.
[15] W. Lu, S. Xiong, K. Xie, Y. Pan, C. Zheng, Identification of solid electrolyte interphase formed on graphite electrode cycled in trifluoroethyl aliphatic carboxylate-based electrolytes for low-temperature lithium-ion batteries, Ionics, 22 (2016) 8.
[16] Y. Cao, N. Tian, D. Bahr, P.D. Zavattieri, J. Youngblood, R.J. Moon, J. Weiss, The influence of cellulose nanocrystals on the microstructure of cement paste, Cement and Concrete Composites, 76 (2016) 10.
[17] I. Valov, R. Waser, J.R. Jameson, M.N. Kozicki, Electrochemical metallization memories—fundamentals, applications, prospects, Nanotechnology, 22 (2011).
[18] W. Hu, X. Chen, G. Wu, Y. Lin, N. Qin, D. Bao, Bipolar and tri-state unipolar resistive switching behaviors in Ag/ZnFe2O4/Pt memory devices, Applied Physics Letters, 101 (2012).
[19] M. Tatsumisago, Y. Shinkuma, T. Minami, Stabilization of superionic α-Agl at room temperature in a glass matrix, Nature, (1991) 2.